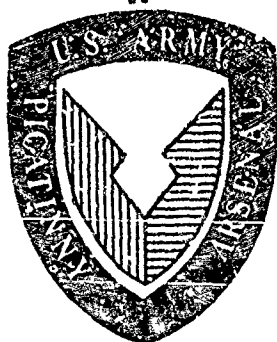TECHNICAL REPORT 4345

A SURVEY

OF THE

PHYSICS OF SHOCK WAVES IN SOLIDS
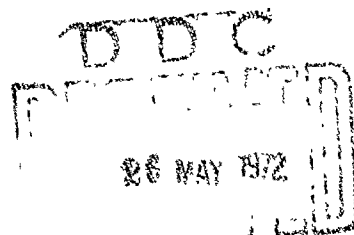
PAUL HARRIS

FEBRUARY 1972

APPROVED FOR PUBLIC RELEASE: DISTRIBUTION UNLIMITED.

PICATINNY ARSENAL

DOVER, NEW JERSEY

DOCUMENT CONTROL DATA - R & D

(Security classification of title, body of abstract and indexing annotation must be entered when the overall report is classified)

1. ORIGINATING ACTIVITY (Corporate author)	2a. REPORT SECURITY CLASSIFICATION
U. S. Army, Picatinny Arsenal, Dover, New Jersey 07801	Unclassified
	2b. GROUP N/A

3. REPORT TITLE

A Survey of the Physics of Shock Waves in Solids

4. DESCRIPTIVE NOTES (Type of report and inclusive dates) The concept of shock wave physics in solids is generalized to include thermal shocks, electromagnetic shocks, and mass density shocks.

5. AUTHOR(S) (First name, middle initial, last name)

Paul Harris

6. REPORT DATE	7a. TOTAL NO. OF PAGES	7b. NO. OF REFS
February 1972	42	73

8a. CONTRACT OR GRANT NO. N/A	9a. ORIGINATOR'S REPORT NUMBER(S)
b. PROJECT NO	Technical Report 4345
c.	9b. OTHER REPORT NO(S) (Any other numbers that may be assigned this report)
d.	N/A

10. DISTRIBUTION STATEMENT

Approved for public release; distribution unlimited.

11. SUPPLEMENTARY NOTES	12. SPONSORING MILITARY ACTIVITY
	U. S. Army, Picatinny Arsenal, Dover, NJ

13. ABSTRACT

The concept of shock wave physics in solids is generalized to include thermal (second sound) shocks, electromagnetic shocks, as well as the more generally understood mass density shocks. It is speculated that thermal shocks may be made to occur in room temperature metals by causing a high power pulsed laser to impact on the metal surface. A laser pulse width of 10^{-12} seconds is derived for the effect to occur.

The state-of-the-art with respect to understanding the compaction behavior of porous materials, the microscopic explanation of electromechanical effects (shock polarization) in a variety of media, and the state of our understanding of the physics of the detonation process is discussed.

DD FORM 1473 REPLACES DD FORM 1473, 1 JAN 64, WHICH IS OBSOLETE FOR ARMY USE.

Unclassified
Security Classification

14 KEY WORDS	LINK A		LINK B		LINK C	
	ROLE	WT	ROLE	WT	ROLE	WT

TECHNICAL REPORT 4345

A SURVEY OF THE PHYSICS OF SHOCK WAVES
IN SOLIDS

BY
PAUL HARRIS

FEBRUARY 1972

Approved for public release; distribution unlimited.

PICATINNY ARSENAL
DOVER, NEW JERSEY

1

TABLE OF CONTENTS

LIST OF ILLUSTRATIONS

LIST OF TABLES

ABSTRACT

The concept of shock wave physics in solids is generalized to include thermal (second sound) shocks, electromagnetic shocks, as well as the more generally understood mass density shocks. It is speculated that thermal shocks may be made to occur in room temperature metals by causing a high power pulsed laser to impact on the metal surface. A laser pulse width of 10^{-12} seconds is derived for the effect to occur.

The state-of-the-art with respect to understanding the compaction behavior of porous materials, the microscopic explanation of electro-mechanical effects (shock polarization) in a variety of media, and the state of our understanding of the physics of the detonation process is discussed.

I. INTRODUCTION

The decades following the outbreak of the second world war have seen the subject of shock wave physics become more than just a large amplitude step-child of hydrodynamics. Shock wave phenomena are now known to be important to solar physics[1], astrophysics[2], possible controlled fusion mechanisms[3,4], solid-state physics[5,6], the physics of explosives[7,8], supersonic flight, and a host of modern military applications[9].

Prior to the second world war shock wave effects were treated in a typical course[10] on hydrodynamics "merely for the reason that all actual fluids are more or less compressible". We can appreciate the growth of the subject of shock wave physics by realizing that where many phenomena are concerned we consider linear physics merely because it represents the limiting case of what we really wish to study. Further, where hydrodynamics dealt exclusively with mass flow, present shock wave physics is much more general; we shall be concerned also with shock waves associated with the propagation of temperature waves[12] (in the absence of a mass disturbance), and shock waves associated with the propagation of electromagnetic waves[13] in a medium of field permittivity and susceptibility. In addition hydrodynamics as a subject does not consider phenomena on a microscopic level as it is a combination of continuum mechanics plus thermodynamics. In shock wave physics we have become very much aware of the role of microscopic mechanisms on the observed macroscopic observables[14].

II. A UNIFIED APPROACH

That a propagating disturbance takes the form of a shock is a consequence of the equation of state appropriate to the material in question and the type of disturbance being studied. In general, from a systems point of view, a nonlinear response-stimulii relation can give rise to shock like phenomena.

For a mass density change propagating into a fluid, the shock velocity U_s is given by [15]

$$U_s = \sqrt{\frac{\rho_i}{\rho_f}\left(\frac{P_f - P_i}{\rho_f - \rho_i}\right)} \tag{1}$$

while the propagation velocity for an infinitesmal disturbance with respect to any local equilibrium state of the material is given by the "sound speed"

$$\text{sound speed} = \sqrt{\frac{\partial P}{\partial \rho}} \tag{2}$$

In equations (1) and (2), ρ is density, P is pressure, and the subscripts i and f refer to before and after the shock, respectively. If in the above we think of ΔP as being the stimulus and $\Delta \rho$ as the response, then, before further detailed consideration of shock propagation, it seems worthwhile to generalize equations (1) and (2) to other systems. Table I demonstrates the generalization.

TABLE I

GENERALIZATION OF STIMULUS AND RESPONSE

Stimulus	Response
(1) Pressure Change, ΔP	Density Change, $\Delta \rho$
(2) Temperature Change, ΔT	Entropy Change, ΔS
(3) Electric and Magnetic Field Changes, ΔE and ΔH	Changes in the induced fields ΔD and ΔB

Where the three systems given in Table I are these which will be considered in some detail here, they do not exhaust the relevant possibilities; a non-linear current-voltage relationship can give rise to shock effects which are of practical importance to transmission line theory[13] or D. C. to A. C. converters utilizing semiconductor materials[16, 17].

Based upon equations (1) and (2), and Table I, we might expect the local "sound" velocities and shock velocities to be given by:

<u>Entropy Propagation</u>: Sound velocity[18] $\propto \sqrt{\dfrac{\partial T}{\partial S}}$, (3)

$$\text{Shock velocity} \propto \sqrt{\frac{T_f - T_i}{S_f - S_i}} . \qquad (4)$$

<u>Electromagnetic Propagation</u>:

$$\text{Sound velocity}[19] \propto \sqrt{\frac{\partial E}{\partial D} \frac{\partial H}{\partial B}} , \qquad (5)$$

$$\text{Shock velocity} \propto \sqrt{\left(\frac{E_f - E_i}{D_f - D_i}\right)\left(\frac{H_f - H_i}{B_f - B_i}\right)} . \qquad (6)$$

In equations (3) to (6) inclusive, $\propto$ means proportional to; the generalization leading to the equations does not guaranty that numerical constants or other factors will not appear in the exact equations.

To the large majority of those involved in shock wave physics, the inclusion of phenomena other than that associated with a propagating mass discontinuity requires some explanation. There are three strong reasons for the generalization we are making, and they are given below:

a. Both the thermal and electromagnetic shocks get coupled to the mass density, so that the thermal and electromagnetic shocks can give rise to the more famila. mass density discontinuity. The thermal expansion coefficient is a coupling coefficient for the thermal shock, while charge density (which is made up of ions and electrons), current density, and bulk polarization couple the field terms in Maxwell's equations with the mass flow.

b. A modern method of introducing a propagating mass discontinuity is to irradiate a target material with a pulse of high energy electrons[20], or a pulse of photons (e. g. , from a laser beam). We will predict in this report that a sharp discontinuity in thermal energy deposition, for example with skin depth rise time as occurs with a laser pulse, can give rise to a temperature (entropy) shock in addition to usual mass discontinuity which results from thermal pressure. Pressure is equivalent to energy density. Since the mass discontinuity and thermal discontinuity propagate at different velocities, the neglect of the temperature shock could cause an error in estimating transport associated with the mass discontinuity.

c. The formalism for the three different shock phenomena listed in Table I are essentially the same, even to employing characteristics in seeking mathematical solutions[13, 21]. In addition, the phenomena are essentially the same although particular mechanisms are different; jump conditions, viscosity, and nonlinear equations of state are all applicable to each phenomena.

The Electromagnetic Shock - Let us consider the two time varying Maxwell's equations for electromagnetic field propagation in a medium.

$$\vec{\nabla} \times \vec{H} = \frac{4\pi}{c} \vec{J} + \frac{1}{c} \frac{\partial \vec{D}}{\partial t} \tag{7}$$

$$\vec{\nabla} \times \vec{E} = -\frac{1}{c} \frac{\partial \vec{B}}{\partial t} \tag{8}$$

where gaussian units have been used[22], c is the velocity of light in vacuum, $\vec{J}$ is current density, $\vec{E}$ is the electric field vector, $\vec{H}$ the magnetic field vector, $\vec{D}$ and $\vec{B}$ are the corresponding induced vector fields, $\vec{\nabla}$ is the gradient operator, and ($\vec{\nabla} \times \vec{H}$) denotes the usual "curl of $\vec{H}$".

We now restrict ourselves to the one dimensional strain type of problem, and allow for spatial variation only in the Z (or X_3) direction. Further restricting ourselves to the special case $\vec{J} = 0$ gives

$$-\frac{\partial H_2}{\partial X_3} = \frac{1}{c}\frac{\partial D_1}{\partial t} \quad \text{and} \quad \frac{\partial H_1}{\partial X_3} = \frac{1}{c}\frac{\partial D_2}{\partial t} , \tag{9}$$

$$-\frac{\partial E_2}{\partial X_3} = -\frac{1}{c}\frac{\partial B_1}{\partial t} \quad \text{and} \quad \frac{\partial E_1}{\partial X_3} = -\frac{1}{c}\frac{\partial B_2}{\partial t} . \tag{10}$$

Here the subscripts 1, 2, and 3 refer to components along the X, Y, and Z directions, respectively. If we assume a steady propagating shock, with the velocity U_s, then we can write $dx_3 = U_s\,dt$. With respect to an observer on the propagating front the first equation of equation (9) and the second equation of equation (10) become, respectively,

$$- dH_2 \quad \frac{U_s}{c} \quad dD_1 , \tag{11}$$

$$dE_1 = -\frac{U_s}{c}\,dB_2 . \tag{12}$$

Integrating equations (11) and (12) across the shock front gives

$$- \{H_2\} \quad \frac{U_s}{c} \quad \{D_1\} , \tag{13}$$

$$\{E_1\} = -\frac{U_s}{c}\,\{B_2\} , \tag{14}$$

where $\{E_1\}$ indicates the jump (i. e., change) in the quantity E_1 across the shock front. Combining equations (13) and (14) yields

$$U_s = c\sqrt{\frac{\{E_1\}\,\{H_2\}}{\{D_1\}\,\{B_2\}}} . \tag{15}$$

For the propagation velocity of small amplitude disturbances in E_1 and H_2 within the large field region where ϵ and μ are to be considered constants, we can form the wave equation

$$\frac{\partial^2 E_1}{\partial x_2^2} = \frac{\mu \epsilon}{c^2} \frac{\partial^2 E_1}{\partial t^2} \tag{16}$$

Equation (16) follows directly from operating on equations (9) and (10). Thus,

$$\text{sound speed} = \frac{c}{\sqrt{\mu \epsilon}} = c \sqrt{\frac{\partial E_1}{\partial D_1} \frac{\partial H_2}{\partial B_2}} \ . \tag{17}$$

We thus see that the formalism for the electromagnetic shock corresponds, as expected, to the formalism for a propagating mass discontinuity as expressed in equations (1) and (2).

If we now include a nonvanishing current density, then equation (11) becomes

$$- dH_2 = \frac{4\pi}{c} J_1 dx_3 + \frac{U_s}{c} dD_1 \ , \tag{18}$$

while equation (12) remains unchanged. The shock velocity thus becomes

$$U_s = c \sqrt{\frac{\{E_1\} \left[\{H_2\} + \frac{4\pi}{c} \int\limits_{\text{shock}} J_1 dx_3 \right]}{\{D_1\} \{B_2\}}} \ , \tag{19}$$

where the integration is carried out over the shock front to the points where the jump values are observed. It is not at all surprising that J_1 enters into equation (19) as it does; currents are always associated with their surrounding magnetic fields. In evaluating equation (19) particular models must be considered as the current density is dependent upon the field variables.

The current density plays the same role in the electromagnetic shock that the flow gradient viscosity plays in a mass shock, namely the smoothing of the discontinuity. The current density, through the electrical conductivity of the material, gives rise to a viscosity and associated penetration depth[23]. Thus, the presence of current density competes against the nonlinearity in ϵ and μ in establishing the thickness of the shock front. Thus, the picture is a large amplitude plane wave electromagnetic pulse (for example a step function) is by some means caused to impinge upon a solid and propagate through it. Inertial effects are coupled to the electromagnetic pulse via the ion and electron current densities which make up J_1. After the pulse has propagated into the medium of finite distance we expect a steady state to be reached with the rise time of the shock being controlled as mentioned above.

The Second Sound Shock - Second sound is typically a low temperature phenomena, and is usually associated with the superfluid state of liquid helium. In the two fluid models for liquid helium the mass density is broken down into "normal" and "superfluid" parts

$$\rho = \rho_s + \rho_n , \tag{20}$$

where the subscripts s and n refer to the two parts mentioned above. It is obvious from equation (20) that ρ_s and ρ_n can be simultaneously varied in such a way that keeps the total mass density constant. The physical mechanism for varying the ratio $\dfrac{\rho_s}{\rho_n}$ is temperature change, with $\rho_n \longrightarrow 0$ as $T \longrightarrow 0\,°K$.

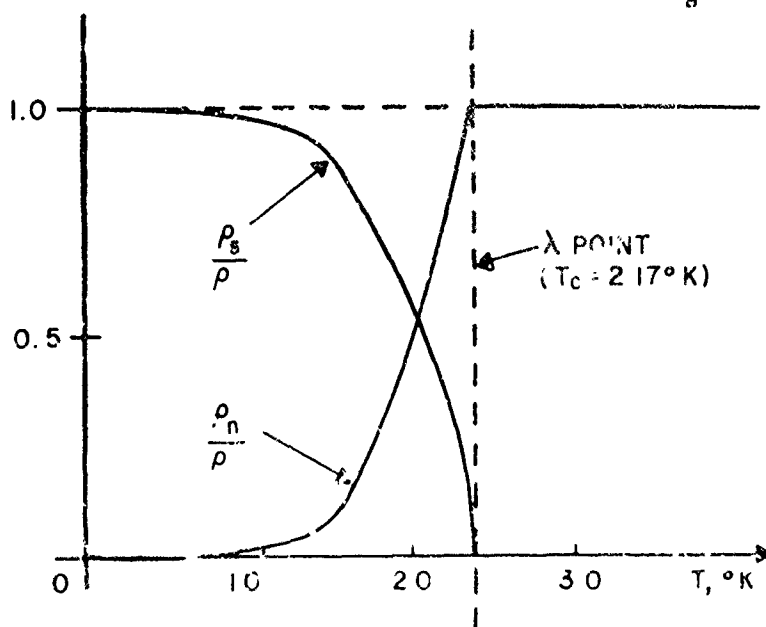Figure 1 gives the temperature dependence of ρ_s and ρ_n.

Figure 1 - The temperature dependence of ρ_s and ρ_n for liquid helium.

In the two fluid models for liquid helium the superfluid component has zero entropy, while the normal component has the usual thermal excitations of a dense gas or liquid with accompanying disorder and entropy. Since $(\rho_s + \rho_n)/\rho$ in figure 1 has the property of equaling unity (i. e., one) a temperature change stimulus will cause an entropy change response without any corresponding change in mass density.

Under the more everyday conditions of heat flow a temperature gradient causes no propagating entropy response, and heat flow takes place instantaneously (i. e., with an infinite propagation velocity[7]) as described by the Fourier equation of heat conduction. For liquid helium below the critical temperature of $2.17°$K, however, a propagating entropy response exists. Such a phenomenon was first observed by Peshkov[24]. The difference between the liquid helium case and the more everyday heat conduction by diffusion case is found in the difference between the thermal diffusivities (this point is expanded upon later in this report). In turn, the difference in diffusivities is related to the difference in specific heats and thermal conductivities.

Considerable experimental and theoretical work has been carried out since the original Peshkov experiments, and it is now an everyday occurrence for a second sound paper to appear in Physical Review Letters, the Physical Review, or a similar journal. The detailed physics[12, 25] of second sound, second sound attenuation, and second sound shock has long since been considered.

To lowest order the conservation of momentum combined with the conservation of entropy can be shown[12, 25] to lead to the wave like equation

$$\frac{\partial^2 S}{\partial t^2} = \frac{\rho_s}{\rho_n} \, S^2 \left[\left(\frac{\partial T}{\partial \rho} \right)_S \nabla^2 \rho + \left(\frac{\partial T}{\partial S} \right)_\rho \nabla^2 S \right] , \qquad (21a)$$

where

$$\nabla^2 = \vec{\nabla} \cdot \vec{\nabla} = \frac{\partial^2}{\partial x^2} + \frac{\partial^2}{\partial y^2} + \frac{\partial^2}{\partial z^2} \qquad (21b)$$

For an ideal second sound ($\nabla^2 \rho = 0$) disturbance propagating in the z direction, and without any variation in the x and y directions, equation (21a) becomes

$$\frac{\partial^2 S}{\partial t^2} = \frac{\rho_s}{\rho_n} S^2 \left(\frac{\partial T}{\partial S}\right)_\rho \frac{\partial^2 S}{\partial z^2} . \tag{22}$$

One thus predicts a second sound velocity, U_2, of

$$U_2 = S \sqrt{\frac{\rho_s}{\rho_n} \left(\frac{\partial T}{\partial S}\right)_\rho} \tag{23}$$

in agreement with the general ideas which went into equation (3). Early theoretical predictions by Landau (1941) give[7, 12, 25] a low temperature limit of U_2 of

$$\lim_{T \to 0°K} U_2 = \frac{U_1}{\sqrt{3}} , \tag{24}$$

where U_1 is the velocity of ordinary or first sound (i. e., the velocity of equation (2) at constant entropy). It is now known[12, 25] that for $T \leq 0.5°$K, U_2 actually rises above the value given by equation (24) and may be due to mean free path effects.

To lowest order when the conservation of entropy and the conservation of momentum are combined with a pure phonon[26] field (i. e., no anharmonic effects or other excitations such as rotons[27]) one arrives[12] at a sound velocity given by equation (24). Anharmonic effects are, however, expected to be present in liquid helium at any finite temperature (after all it is a liquid the nucleii of which are not in definite equilibrium positions). Roton states are also occupied. The anharmonic effects plus excitations such as rotons leads to deviations in the relevant equation of state (i. e., ˉ vs S). These deviations take the form of nonlinearities which in turn lead to an amplitude (i. e., temperature change) dependent second sound velocity through equation (23).

The effect of the above mentioned nonlinearity on a propagating thermal pulse for temperatures near but below and above 1.9°K is shown in figures 2a and 2b, respectively.
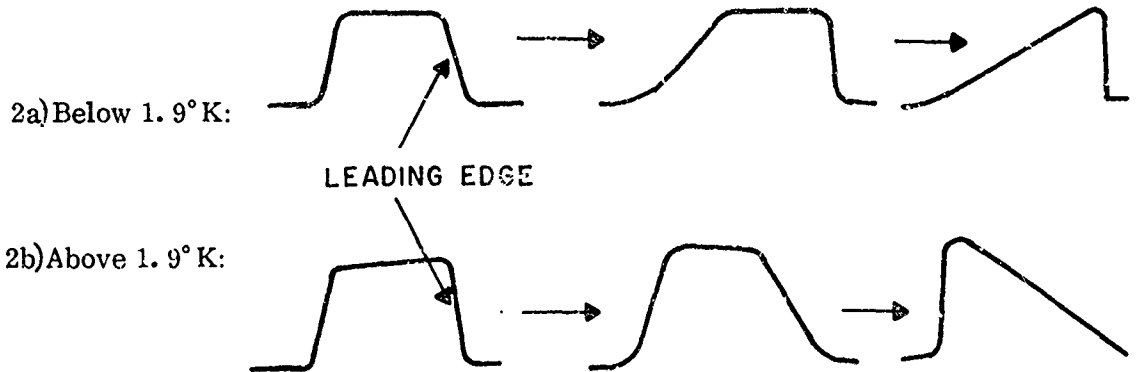
2a) Below 1.9°K:

LEADING EDGE

2b) Above 1.9°K:

Figure 2: The propagation of second sound pulses of large amplitude in liquid helium (a) below 1.9°K, and (b) above 1.9°K. From Atkins[12].

The shock effect shown in figure 2 is based upon experiments by Osborne[28]. The situation depicted for below 1.9°K would seem to correspond to the usual case of a propagating mass discontinuity where a compressive wave front shocks up. The above 1.9°K situation would seem to correspond to the infrequently observed propagating mass discontinuity case where a rarefaction wave front shocks up. The cases (a) and (b) of figure 2 require, respectively

$$\frac{\partial^2 T}{\partial S^2} > 0 \quad \text{and} \quad \frac{\partial^2 T}{\partial S^2} < 0 ,$$

which correspond to $\frac{\partial^2 V}{\partial \rho^2} > 0$ and $\frac{\partial^2 V}{\partial \rho^2} < 0$, respectively for compressive and rarefaction mass discontinuity shocks[29].

We have seen that second sound and second sound shocks exist in liquid helium. Our more general arguments, which are illustrated in Table I, would indicate that more everyday materials might as well be expected to exhibit the phenomena. Chester[30] predicts second sound in the more everyday materials providing that relaxation time and applied frequency conditions are fulfilled. Chester notes that the Fourier heat equation is really an approximation to

$$\tau \frac{\partial \vec{q}}{\partial t} + \vec{q} = -K\vec{\nabla}T , \tag{25}$$

where $\vec{q}$ is the thermal current density, τ is a relaxation time, and K the coefficient for thermal conductivity. When equation (25) is combined with the continuity equation for heat transport, below,

$$C \ \frac{\partial T}{\partial t} + \vec{\nabla} \cdot \vec{q} = 0 \tag{26}$$

then we arrive at the modified wave equation

$$\frac{\partial^2 T}{\partial t^2} + \frac{1}{\tau} \ \frac{\partial T}{\partial T} \ .. \frac{K}{} \ \nabla^2 T = 0 \tag{27}$$

In the above, C is the heat capacity per unit volume. From equation (25) we see that in the limit $\tau \rightarrow 0$ we arrive at the usual Fourier heat equation.

We would now like to explain the physics of equation (25). Consider the temperature distribution shown in figure 3 below. Plane geometry is assumed.
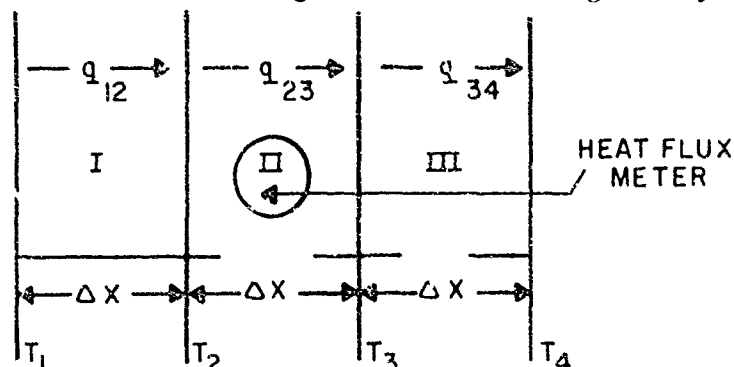
Figure 3 – A spatial temperature distribution and corresponding heat fluxes. Center region is the region of observation.

Allow a heat flux meter to be set up somewhere between the temperature planes T_2 and T_3. Further, if ℓ is the transporting particles (or quasi-particles) mean free path, let $(\Delta x) \sim \ell$. We ask ourselves what the flux meter measures as a function of time if a switch is thrown at time t = 0 which changes the temperature distribution from a homogeneous one to in which

$$T_1 - T_2 > T_2 - T_3 > T_3 - T_4 \ ,$$

and further that the new temperature distribution is maintained for all time. At time $t = 0$ the meter measures q_{23} which is the result of the local temperature distribution $(T_2 - T_3)/(\Delta x)$. If c is the velocity of the transporting particles then the flux meter measures, in addition to q_{23}, flux contributions from regions I and III after a time $t \sim \ell/c$. For times $t > \ell/c$ the flux must approach a steady state constant value for a constant temperature distribution. Clearly then a nonconstent temperature gradient gives rise to a time varying flux. We thus see that $t = 0$ in equation (25) will not explain the above expected observations.

In the above paragraph we have seen that the flux contribution, Δq, from regions I and III is of the form

$$\Delta q \propto \ell \, \frac{\partial^2 T}{\partial x^2} \, . \tag{28}$$

For transporting velocity c equation (28) can be rewritten as

$$\Delta q \propto \frac{\ell}{c} \, \frac{\partial}{\partial t} \left(\frac{\partial T}{\partial x} \right) , \tag{29}$$

or using the first order effect $\vec{q} = - K \vec{\nabla} T$ in equation (29)

$$\Delta \vec{q} \propto \tau \, \frac{\partial \vec{q}}{\partial t} \, . \tag{30}$$

We thus have a physical understanding of the origin of the relaxation term in equation (25). Weymann[31] arrives at the relaxation time modified heat conduction equation by considering the linear random walk problem.

To now we have been only considering what may be called phonon second sound. It may be possible that electrons and holes in metals[32] and semiconductors[33] will support similar macroscopic thermal oscillations.

Let us now consider equation (27) in some detail. Whether or not finite velocity propagating solutions are allowed depends upon the relative magnitudes of the two terms having derivatives with respect to the time. Clearly if the second derivative term dominates the first derivative term equation (27) can be approximated by the wave equation. If T is of the form $T = T_0 (\hat{r}) \exp (i\omega t)$, then wavelike solutions hold in the limits $\omega \to \infty$ and/or $\tau \to \infty$, or collectively $\omega\tau \geq 1$.

To further estimate the values of ω and τ necessary for wavelike solutions let us write equation (27) in the form

$$\frac{1}{v^2} \frac{\partial T}{\partial t^2} + \frac{1}{\chi} \frac{\partial T}{\partial t} - \nabla^2 T = 0, \tag{31}$$

where $v = \left(\frac{K}{\tau C}\right)^{1/2}$ is a velocity, and $\chi = \frac{K}{\rho C_m}$ is the thermal diffusivity

with C_m the specific heat (heat capacity per unit mass). The condition for wavelike solutions then becomes

$$\frac{v^2}{\omega\chi} \lesssim 1. \tag{32}$$

Let us apply equation (32) to an ordinary material such as room temperature aluminum. For v we take the velocity of ordinary (i.e., first) sound, say 6×10^5 cm/sec. and $\chi = 1$ cm^2/sec. Thus for room temperature aluminum we expect that $\omega \gtrsim 3.6 \times 10^{11}$ radians/sec, or a frequency greater than 5×10^{10} cycles/sec, is necessary for thermal wave propagation. The relaxation time τ is actually the time for energy or momentum loss (i.e., the relaxation time for the so called "Umklapp" processes[34]). Since we must have local thermal equilibrium, we must also satisfy the requirement $\omega\tau_N < 1$ in order to propagate a thermal wave. Here τ_N is the relaxation time for momentum conserving phonon collisions (i.e., the so called "normal" processes[34]). Thus, there is a window[35] for thermal wave propagation given by

$$\frac{1}{\tau} \lesssim \omega \leq \frac{1}{\tau_N} \tag{33}$$

An applied thermal frequency of approximately 6×10^{11} radians per second falls within the window given by equation (33).

Because of the above results we are led to believe that a high energy laser pulse, impinging on a slab of aerospace material, will result in energy leaving the skin depth material via a propagating thermal pulse. Such a thermal pulse would be in addition to energy also leaving via the propagating mass discontinuity which results from the pressure gradient accompanying the energy deposition in the skin depth area. The energy carried off by the thermal pulse relative to that of the propagating mass discontinuity is a question yet to be determined, but it is quite obvious that the thermal pulse is not to be neglected off hand.

III. MASS DENSITY SHOCKS

Propagating mass density discontinuities are generally what people have in mind when they speak of "shock waves". The general theory of mass shocks has long since been written down (e. g. , see references 7, 21, and 36) and understood. As distinct from the general theory, the state-of-the-art of mass shocks is concerned with effects which occur in special classes of materials and under special conditions. The question with respect to these effects is to arrive at a model which will explain the experimental observations.

In terms of state-of-the-art, this report treats mass shocks in porous solids, various mass shock electromechanical effects, and mass shocks in energetic materials (i. e. , explosives). As areas of investigation they represent a large part of the current interest in "shock" wave physics. For the remainder of this report, by shock we shall mean a mass shock.

There are three ways to cause a shock wave to occur in a material. An already existing shock in one medium can be propagated into a second material simply by having the two materials be in contact. Solids can be caused to impact each other at high velocity resulting in shock waves propagating out from the point of impact. Lastly, thermal energy can be stored in a material in a spatially inhomogeneous manner, since thermal energy is equivalent to a pressure, and since $\frac{\partial P}{\partial x}$ is equivalent to a force per unit volume the inhomogeneous energy deposition combined with a nonlinear equation of state will result in a propagating shock.

Porous Solids -   Any Material which has a mass density less than the maximum possible equilibrium mass density at a given pressure and temperature is called a porous solid. Examples of such materials are foams (e. g. , polyurethane), less than normal density explosives and porous metals.

Porous materials are of both engineering and academic interest. Polyurethane foams are utilized as shock mitigators by having the shock energy absorbed in the process of compacting the foam to its normal solid density. Porous metals have engineering applications but are also of extreme academic importance. If a solid of normal density is shock-loaded, its final state lies

in a single curve (the Hugoniot curve) in the PV plane. On the other hand, when a solid such as porous tungsten is shock-loaded, the final state reached will reside on one of a continuum of Hugoniot curves, depending upon the initial porosity; the irreversible processes which occur during compacting yield PVT states for the compacted solid different from those occurring in the shock-loaded material having initial normal density. Thus, by shock-loading an initially porous material to beyond complete compaction, it is possible to investigate broad regions in PVT space. This academic property of porous materials was first pointed out by Zeldovich[37].

Another important application of porous materials is in the area of explosives. It is well known that the initiation sensitivity of explosives to mechanical shock depends upon the final density to which a granular explosive may be pressed[38]. This area also has both academic and engineering applications.

Soviet and Western interest in inert porous materials, judging from the open literature, has been in different pressure regimes. Western interest has been strong in the area of shock propagation in the pressure range at which compaction occurs. On the other hand, the Russians appear to have their main effort in the pressure range beyond which compaction has already occurred. Among the interesting ingredients of high-pressure physics which the Russians have studied via porous materials is the electronic contribution to the Gruneisen constant[36, 39].

Presently the major unknown in the area of porous solid physics concerns the mechanism of the compaction process. In a typical experiment a one-dimensional strain shock (no net local particle displacement perpendicular to the direction of shock propagation) the free surface velocity and an average shock velocity are measured. Then, by using Rankine-Hugoniot type conservation equations[7, 40] (for mass, momentum, and energy flows) the pressure and energy density may be determined[40, 41] in the shocked regime. Alternatively, the porous material may be backed up with a quartz (or other piezoelectric) transducer, to yield pressure and particle velocity[42]. Again, the conservation equations are used to yield shock velocity and energy density.

Thus, experimentally it is possible to catagorize a porous solid according to its gross macroscopic behavior in a shock environment. The motivation for the experiments usually is to arrive at or to verify a proposed equation of state in the dynamic regime. Such an equation of state is generally of the form

$$P = P (\rho, \rho_s, T, \mathcal{E}, t) \qquad (34)$$

where ρ is the actual local mass density. ρ_s is the mass density for the material if it voidless but otherwise in the same state as the solid under consideration, and $\mathcal{E}$ is the internal energy density. The time dependence is meant to include strain rate effects.

The type of porous material equation of state modeling which has so far occurred centers on choosing particular functional forms (or conceptual physical models) which correspond to equation (34). One can think of the existing modeling as belonging to three different classes.

a. The locking solid model[43]. In this model the P versus ρ dependence is basically taken as shown in figure 4. Variations in the model are achieved by allowing the compacted material to be more or less compressible, and by allowing the yield strength to be more or less significant.
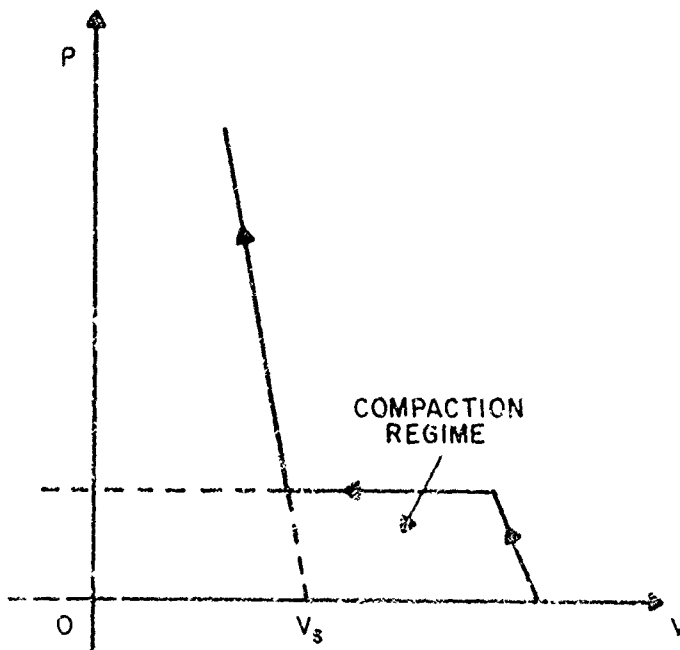

Figure 4 - The locking model for porous solid compression. Y is the
yield stress and V_s is the volume of the original undeformed
material were it voidless

b. The P-α model[44]. Whereas the locking model, as shown in figure 4, has $\alpha \equiv \dfrac{\rho_s}{\rho}$ independent of pressure in the compaction regime, the P-α model gives α an explicit pressure dependence. In particular, if one assumes a polynominal expansion for α

$$\alpha = \alpha_0 + \alpha_1 P + \alpha_2 P^2 + \alpha_3 P^3 + \cdots , \qquad (35)$$

then suitable boundary conditions on α and $\dfrac{d\alpha}{dP}$ (evaluated at the yield and fully compacted points in the P-ρ plane) are sufficient[44] to determine α_0, α_1, α_2, and α_3.

c. The plate – air gap model[45]. In this model the porous material is viewed as plates of solid material (the solid matrix of the porous medium) separated by air gaps (corresponding to the voids). A 1-D strain shock propagates via the plates being transported across the air gaps, in effect collapsing the voids, and thus resulting in a voidless material behind the shock front.

The locking solid model and the P-α model have in common that they are basically empirical equation of state models. They are not based upon the microscopic details of the porous solid structure in the spirit of arriving at an equation of state of a crystalline solid via a knowledge of interatomic potential[36]. On the other hand the plate-air gap model, including more sophisticated versions of it[46], is based upon a macroscopic equivalent of a microscopic model.

While each of the models mentioned above is capable of predicting shock velocity and attenuation, none of them are capable of predicting either the rise time (and thus shape) of an elastic precursor or the main compaction wave. While an attempt has been made[47] to include a stress relaxation term within the P-α model, to now the approach has only been empirical and the fitted relaxation times have no obvious relation with respect to the actual details of void collapse[48].

In order to really understand the compaction process in porous materials it seems necessary to first consider the detailed deformation mechanics of individual voids in a representative matrix material and then to develop suitable methods of averaging over the entire material. With such an approach the necessary time dependent constitutive equations (i.e., explicit strain rate dependence), the shock velocity, attenuation, and wave shapes would automatically result. The approach has already been successful for shock calculations in solids having dislocations[49].

Energy deposition experiments (one of the three methods of shock generation previously mentioned) in porous solids have shown some interesting effects. It has been found experimentally[42, 50] that the Gruneisen constant of porous solids is very much dependent upon the degree of porousity. The Gruneisen constant, Γ, is defined thermodynamically as

$$\Gamma = \frac{1}{\rho} \left(\frac{\partial P}{\partial \varepsilon} \right)_\rho \tag{36}$$

where the derivative is to be evaluated at constant density. Table II below gives some of the experimental data for porous PETN obtained by using an electron beam to deposit energy in the material. Although some of the data shown in Table II have very large errors, the trend as a function of ρ_o / ρ_{so} is clearly discernible.

<div align="center">

TABLE II[a]

ENERGY DEPOSITION PROPERTIES OF PETN

</div>

ρ_o / ρ_{so}[b]	Density gm/cm^3	Sound Speeds cm/sec x 10^{-5}	Effective Γ
0.95	1.67	2.8	1.2
0.90	1.59	2.4 ± 0.1	0.51
0.87	1.54	1.8 ± 0.3	0.15
0.84	1.48	1.7 ± 0.3	(0.07 to 0.23)

[a]This table was taken, with minor changes, from reference 42.
[b]ρ_o is the density of the undeformed porous PETN, while ρ_{so} is the density of undeformed voidless PETN.

24

The experiments of Shea et al[42] resulting in Table II are interesting in that the electron beam was depositing energy for a longer period of time than it takes a sound wave to propagate across a typical particle of the porous PETN material. Consequently, the Γ measured was not the true constant volume Gruneisen parameter as defined by equation (36). Exactly what detailed microscopic physics corresponds to the measured Γ is a very difficult[48] question in porous solid mechanics which remains unanswered. While the measured "effective Γ" is a worthwhile experimental variable in that it characterizes the gross behavior of the material, unforturnately it does not allow for distinguishing between all possible porous materials as a function of material parameters.

Mazella et al[50] have proposed a Gruneisen parameter for a porous material given by

$$\Gamma = \frac{c^2}{c_s^2} \, \Gamma_s \, , \tag{37}$$

where Γ_s is the parameter for the voidless undeformed solid, with c_s being the propagation velocity corresponding to a pure bulk modulus wave[51a] in the voidless undeformed material. c is the corresponding velocity for the porous solid. Equation (37) follows from the assumed[50] form for the equation of state in differential form

$$dP = - K \, \frac{dV}{V} + \left(\frac{K}{K_s}\right) \, P_s \, \Gamma_s \, (\Delta \varepsilon) \, , \tag{38}$$

where K denotes bulk modules. Equation (38) differs from the equation of state of a voidless material by the presence of the factor $\frac{K}{K_s}$. Physically the factor $\frac{K}{K_s}$ spreads the energy which the electron beam has deposited in the solid particles of the porous material over the entire solid. To see this consider

$$K = V \, \frac{\partial P}{\partial V} = V \, \frac{(\Delta P)}{(\Delta V)}^* \, , \qquad K_s = V_s \, \frac{\partial P}{\partial V_s} = V_s \, \frac{(\Delta P)^*}{(\Delta V_s)} \, , \tag{39}$$

25

where $(\Delta P)^*$ indicates an equal differential pressure to porous and voidless media having the same solid composition. By combining the energy density term of equation (38),

$$\Delta P = \frac{K}{K_s} (\Delta P)_s , \tag{40}$$

with equation (39) we find

$$(\Delta P) = \frac{\epsilon_s}{\epsilon} (\Delta P)_s \text{ or } \epsilon (\Delta P) = \epsilon_s (\Delta P)_s , \tag{41}$$

where ϵ_s is the strain in the voidless material for the incremental $(\Delta P)^*$. The second equation (41) is the energy statement alluded to above.

It thus appears that equation (37) is valid for those experimental situations where the energy deposition is so long in time that the porous medium is able to continuously adjust its density on a microscopic scale without effecting the macroscopic density. In some experimental cases equation (37) is found to hold, and in others not to hold[50]. Unfortunately we are not given sufficient information about the materials examined (e. g. , particle size) to judge the theoretical applicability of equation (37) via equation (41). Even though we expect a time dependent compaction process, equation (37) does not contain a relaxation time.

Electromechanical Effects - Experimentally it is well known that electrical signals originate in many materials when a shock wave is caused to propagate through the material. No external source of electric power is necessary for the existence of such signals. A typical experimental arrangement for the effect in question is shown in figure 5.

An obvious example of a specimen material is quartz, because of its piezoelectric character. The effect in quartz is so well understood that quartz is used as a gauge[51h] to measure shock amplitudes in many experiments. On the other hand, many materials which are not piezoelectric (some have highly symmetric crystal structures) also yield electrical signals upon shock loading. The alkali-halides[52], and germanium and silicon[53] are examples of non-piezoelectrics in which the effect is seen. Indeed, even plastics[54] yield signals.

High
Explosive
Plane Wave Shock
Generator

Specimen
Material

A = Ammeter

V = Voltmeter

R_L = Load Resistor
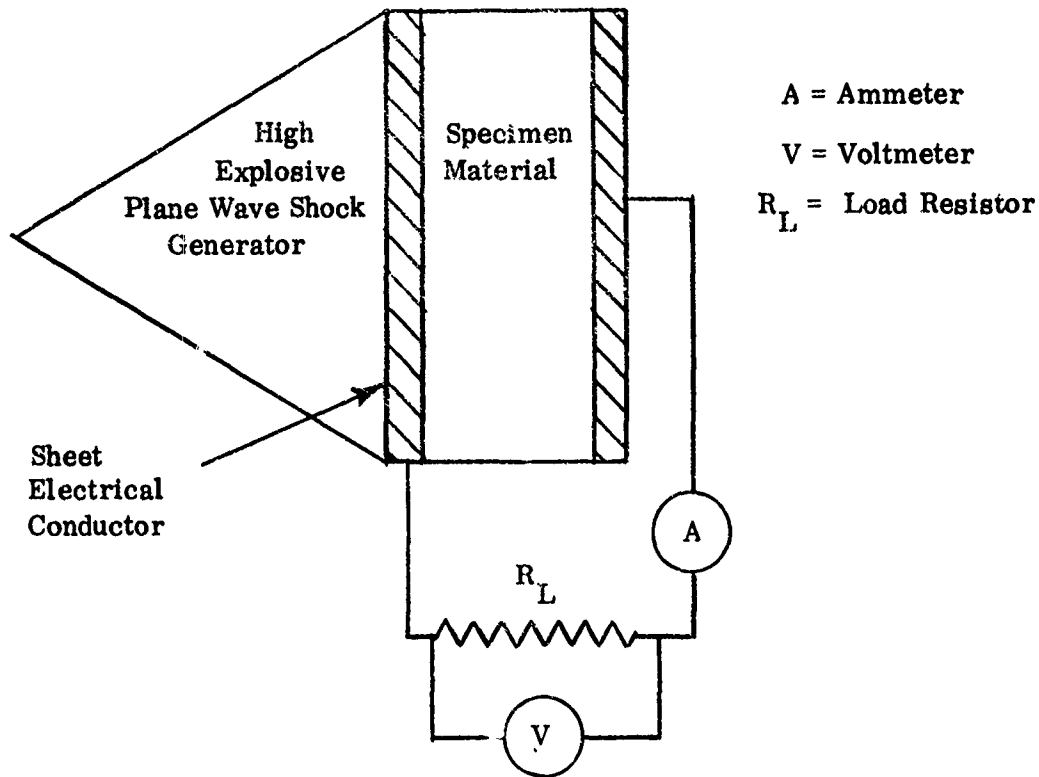
Sheet
Electrical
Conductor

R_L

A

V

FIGURE 5 – Typical Experimental Arrangement for Measuring
Shock Induced Electrical Effects

There also is an interesting related effect known[55] as the "anomalous thermoelectric effect". Here a thermoelectric junction is shock loaded with the shock propagating perpendicular to the plane of the junction. The observed electrical signal is approximately an order of magnitude larger than that associated with the thermoelectric voltage which would be associated with the compression caused adiabatic temperature rise in the junction materials.

To date explanations for the effect in plastics do not exist. A crude qualitative theory involving dislocation motion has been put forward[56] to explain the shock induced voltages in the centrosymmetric alkali-halides, and first order transport theory has been applied to germanium[57], silicon, and metallic[58] band structures as first attempts which show the theoretical existence of the effects in those materials. The theory for germanium and silicon

is essentially an extension of the so-called "acousto-electric" effect[59] wherein experimentally the effect is seen via acoustic stimulation. The semiconductor predictions are in order of magnitude agreement with the experiments of Mineev et al[53], while the theoretical results for the metallic case are still open to question. For the metallic case Harris[58] predicts approximately 10 microvolts per 100 kilobars of impressed shock, a prediction orders of magnitude smaller than that observed with shocked metallic thermocouple junctions[55].

For the metallic thermocouple junction, Migault and Jacquesson[60] have attempted to explain the anomalis thermoelectric power by invoking a pressure induced force on the conduction electrons. Their treatment, however, does not take into account relaxation time effects within and/or behind the shock front – a physics point which was found to be of paramount importance (i.e., zero voltage if it was neglected) for the case of a single metal[58]. The Migault and Jacquesson results are in order of magnitude agreement with experiment.

Directed to the anomalous thermoelectric power problem, Conze et al[61, 62, 63] have done some very general work concerning electrons and electron-phonon interactions in a shocked solid. Directed towards the "shock polarization" of the alkali-halides, Harris[64] has considered the possibility of the elastic orientation of the Hydroxide-ion impurities which are generally found as unwanted impurities in the as-grown crystals. Such a theory would require a nonsymmetric stress tensor, and make for a very interesting theoretical mechanics problem (in spite of experimental evidence indicating that the effect is unimportant[65]). In addition to the work of Harris[57] for the semiconductor problem, Horie[66] has published work based upon a phonon-drag type of effect which is in the right direction theoretically. Horie believes that his results indicate no measureable signals at room temperature, in contradiction to experiments[53] where results are indeed seen.

The question of shock induced electrical effects in solids is wide open. As of this writing there are not any microscopic theories capable of predicting electrical voltages for arbitrarily large shock amplitude. The best which can be said about the present situation is that some first or second order theories allow one to accept the existence of the shock induced voltages on a theoretical basis. This area of shock physics requires a great deal more detailed theoretical and experimental work to be done before one could feel remotely happy about the situation.

28

<u>Energetic Materials</u> -   Porous materials and electromechanical effects were
considered first in this chapter because both subject areas are considered to
be important to the physics of initiation of energetic materials (explosives).

The fundamental microscopic processes which describe initiation
and detonation, in terms of the parameters which define an undetonated chemical
explosive material are not understood.   Indeed the thermonuclear detonation
wave structure[67] is much better understood than that of the chemical detonation
wave structure.   The reason for the above surprising statement is simple;
nuclear scattering cross sections and processes (millions of electron volts) are
better understood then chemical "scattering" cross sections and processes
(electron volts).   Furthermore, in the electron volt regime the energies con-
tributed by solid state coherent effects are expected to be of importance while no
such statement can be made for the Mev regime.   In other words extended
intramolecular as well as intermolecular effects are expected to be important
in the processes which characterize solid chemical explosives.

Semi-recent literature has contained experimental[68] and theoretical[69, 70]
hints of electromechanical phenomena playing a role in the detonation process.
Unfortunately the type of experiments so far undertaken are not the rigorous
solid state experiments that a theoretical physicist would like to work from.
Rather the experiments point only to the existence of possible ionization phenomena
associated with initiation to detonation.   The theoretical work has to now only
dealt with individual mechanisms (e. g. , graded band gap effects[70]) without
completely carrying the calculations through to detonation physics.   It is
interesting, however, that Williams[70] in effect suggests that an electric dipole
layer may be associated with the detonation front while Mineev et al[53] and Harris[57]
predict a dipole layer to be associated with the shock front in an inert material.

Other approaches to the question of initiation are also taking place.
For example, various groups are studying the crystal structure of solid
explosives via neutron diffraction techniques[71], while some workers are
considering the detailed micromechanics of bond breakage under a plate impact
type of environment[72].   Aside from giving detailed crystallographic information,
there is the possibility that neutron diffraction experiments will lead to the
discovery of a "soft mode" and a consequent lattice instability[73].   Of all the non-
thermal approaches to the question of initiation to detonation, it would appear
that this crystallographic approach is the most rigorous and complete so far
undertaken.

To date the most successful attack on the initiation problem appears to be via the macroscopic thermal route, sometimes called "hot spot" theory. Trott et al[8] have shown that an Ahrenius term such as exp(-A/RT), when combined with adiabatic heating effects resulting from plate impact caused compression, is sufficient to explain the observed nonelectrical phenomena associated with homogeneous and heterogeneous explosives. The success goes so far as to enable the calculation of a reaction or incubation time for detonation to occur at the impacted surface in a homogeneous explosive.

The question of the microphysics pertinent to detonation phenomena, in terms of the parameters which are important to solid state physics, is wide open.

VI. SUMMARY

We have surveyed the field of shock wave physics in solids. In so doing we have generalized the concept of a shock wave to include thermal, electromagnetic, as well as the more generally understood mass density shocks.

We have briefly examined the state-of-the-art with respect to understanding the compaction behaviour of porous materials, the microscopic explanation of electromechanical effects (shock polarization) in a variety of media, and the state of our understanding of the physics of the detonation process. Porous materials, electromechanical phenomena, and detonation physics represent wide open areas for future investigation.

REFERENCES

1. W. H. Bostick et al, in Solar Magnetic Fields (D. Reidei, Dordrecht, 1971), edited by R. Howard. International Astronomical Union Symposium, Paris, France, 1970.

2. V. P. Korobeinikov, Gas Dynamics of Explosions, in Annual Review of Fluid Mechanics, Vol. 3 (Annual Reviews, Palo Alto, 1971).

3. S. Glasstone and R. H. Lovberg, Controlled Thermonuclear Reactions (D. VanNostrand, Princeton, 1960).

4. A. L. Fuller and R. A. Gross, Phys. Fluids 11, 534 (1968).

5. Dynamic shock wave experiments in solids are capable of simultaneously producing the environments associated with static high pressure work and megacycle range ultrasonics. Relaxation phenomena can thus be studied as a function of pressure well into the megabar region. In addition, with present technology it is possible to reach higher pressures in dynamic experiments than in static experiments.

6. D. G. Doran and R. K. Linde, Solid State Physics 19, 229 (1966).

7. L. D. Landau and E. M. Lifshitz, Fluid Mechanics (Addison-Wesley, 1959) Chapter XIV

8. B. D. Trott et al, Impact Sensitivity of Explosives, ARPA Order 854, June 2, 1969. Battlle Memorial Institute, Columbus, Ohio.

9. One possible method of destroying enemy reentry vehicles is supposidely to cause shock waves to be generated in a reentry vehicle's missile skin, causing the ablator to be removed, and resulting in the vehicle burning up as it passes through the atmosphere. See R. L. Garwin and H. A. Bethe, Scientific American 218, 21 (1968).

10. H. Lamb, Hydrodynamics (Dover, New York, 1932), p. 476.

REFERENCES (CONT)

11. See, for example, the Appendix in P. Harris, Phys. Rev. 143, 546 (1966).

12. K. R. Atkins, Liquid Helium (University Press, Cambridge, 1959).

13. L. G. Katayev, Electromagnetic Shock Waves (Iliffe Books Ltd., London, 1966).

14. For example, the temperature distribution in a polyatomic gas, behind the shock front, depends upon exchanging energy between translational, rotational, and vibrational modes. Since detonation in an explosive gaseous mixture requires molecular disassociation and rearrangement, such energy exchange is of vital importance to detonation theory. See D. F. Hornig, Energy Exchange in Shock and Detonation Waves, Princeton University, October 1962. ONR Contract No. 1858(24), NR-061-041.

15. M. H. Rice et al, Solid State Physics 6, 1 (1958).

16. The so-called Gunn effect depends upon "negative differential resistance", which is a nonlinear phenomena, wherein hot electrons are promulgated to a higher energy band of lower mobility. This results in domains of very small dimensions, which on the scale of experiment may be treated as discontinuities, progagating through the crystal specimen at the electron drift velocity. See, for example, E. M. Conwell, High Field Transport in Semiconductors (Academic Press, New York, 1967).

17. The author was privaliged to observe Gunn effect type phenomena in compensated n-type GaAs and Ge while a junior researcher at the Radio Corporation of America Laboratories, Princeton, during the summer of 1959. Unfortunately he did not understand what he saw, and went on to further education and other things rather than become vice president of an industry.

REFERENCES (CONT)

18. The local sound velocity characteristic of entropy propagation is known as second sound, while the more common sound velocity characteristic of a propagating mass density disturbance is called first sound. See references 7 and 12.

19. The velocities given by equations (5) and (6) are really the group velocities for the respective disturbances. If the electromagnetic disturbance was considered to be in a vacuum, then equations (5) and (6) would each be equal to 3×10^{10} cm sec^{-1}.

20. P. W. Spence et al, "Shock Generation in S-200 Beryllium Using a Pulsed Electron Beam". Physics International Company Report PIIR-12-70, February 1970.

21. R. O. Courant and K. O. Friedrichs, Supersonic Flow and Shock Waves (Interscience, New York, 1948).

22. Gaussian units are used here since they are the conventional units of propagating mass discontinuity physics.

23. J. D. Jackson, Classical Electrogynamics (John Wiley and Sons, New York, 1962).

24. V. Peshkov, J. Phys. U. S. S. R. 8, 131 (1944).

25. J. Wilks, Liquid and Solid Helium (Clarendon Press, Oxford, 1967).

26. A photon is a quantized unit of interatomic vibrational energy.

27. A roton is a quantized unit of molecular rotational energy.

28. D. V. Osborne, Proc. Phys. Soc. A, 64, 114 (1951).

29. P. Harris, J. Acoust. Soc. Amer. 40, 226 (1966).

30. M. Chester, Phys. Rev. 131, 2013 (1963).

REFERENCES (CONT)

31. H. D. Weymann, Amer. J. Phys. 35, 488 (1967).

32. R. N. Gurzhi and V. M. Kontorovich, Soviet Physics JETP 28, 577 (1969).

33. R. N. Gurzhi and V. M. Kontorovich, Soviet Physics JETP 33, 644 (1971).

34. J. M. Ziman, Electrons and Phonons (Clarendon Press, Oxford, (1962).

35. R. A. Guyer and J. A. Krumhansl, Phys. Rev. A133, 1411 (1964).

36. V. N. Zharkov and V. A. Kalinin, Equations of State for Solids at High Pressures and Temperatures (Consultants Bureau, New York, 1971).

37. Ya. B. Zeldovich, Soviet Physics - JETP 5, 1103 (1957).

38. M. W. Evans et al, Fourth Symposium on Detonation, 12-15 October 1965, White Oak, Silver Spring, Maryland , p. 258.

39. K. K. Krupnikova, Soviet Physics - JETP 15, 470 (1962).

40. M. H. Rice, R. G. McQueen, and J. M. Walsh, Solid State Physics 6, 1 (1957).

41. R. R. Boade, Experimental Shock Loading Properties of Porous Materials and Analytic Methods to Describe These Properties, SC-DC-70-5052, 1970. Sandia Laboratories, Albuquerque.

42. J. H. Shea, A. Mazella, and L. Avrami in Fifth Symposium on Detonation, Pasadena, California, 18-21 August 1970.

43. See, for example, L. Seaman and R. K. Linde, Distended Material Model Development, Volume 1. Stanford Research Institute, Menlo Park, California. Tech. Report No. AFWL-TR-68-143, Vol. 1.

REFERENCES (CONT)

44. W. Herrmann, J. Appl. Phys. 40, 2490 (1969).

45. J. Thouvenin, in Fourth Symposium on Detonation, U. S. Naval Ordnance Laboratory, Silver Spring, Maryland B, 146 (1965).

46. J. F. Heyda in Behaviour of Dense Media Under Dynamic Pressure (Gordon and Breach, New York, 1968).

47. B. M. Butcher, The Description of Strain Rate Effects in Shocked Porous Materials, Seventh Sagamore Army Materials Research Conference, Raquette Lake, New York, Sept. 1970.

48. P. Harris, The Gruneisen Constant of Porous Materials in Energy Deposition Experiments, Picatinny Arsenal, Dover, New Jersey. Tech. Rept. 4255, August 1971.

49. P. Harris and R. F. Greene, J Appl. Phys. 35, 2170 (1964).

50. A. Mazzella, J. Shea, and T. Stefansky, Dynamic Response of Porous Materials to Electron Beam Deposition. Physics International Co. Report PIFR-216, October 1971.

51a. A pure dilitational wave in a medium of zero rigidity.

51b. R. A. Graham et al, J. Appl. Phys. 36, 1775 (1965).

52. L. G. Doran and T. J. Ahrens, Poulter Laboratories, Stanford Research Institute, Project 4100, Contract DA-04-200-ORD - Final Report, 31 August 1963.

53. V. N. Mineev et al, Soviet Phys. - JETP Letters 5, 244 (1967).

54. E. J. Eichelberger and G. E. Hauver, Les Ondes de Detonation, Publications du Centre National de la Research Scientifique, (Paris 1962), pp 361-381.

REFERENCES (CONT)

55. J. Crosnier et al, Fourth Symposium on Detonation, 12-15 October 1965, White Oak, Silver Spring, Maryland, p. 40.

56. J. Y. Wong et al, J. Appl. Phys. 40, 4137 (1969).

57. P. Harris, Shock Induced Electrical Signals in N-Type Germanium and Silicon. SMUPA-TK-2018, Picatinny Arsenal, Dover, New Jersey. April 1971.

58. P. Harris, Phys. Rev. B, Feb. 1972.

59. G. Weinreich et al, Phys. Rev. 114, 33 (1959).

60. A. Migault and J. Jacquesson in Behaviour of Dense Media Under High Dynamic Pressures (Gordon and Breach, New York, 1968), p. 431.

61. H. Conze et al in Behaviour of Dense Media Under High Dynamic Pressures (Gordon and Breach, New York, 1968), p. 441.

62. H. Conze, Polarization d'un Metal et Creation d'un Champ Electrique Dans une Onde de Choc, Scientific Report S-69-3, Centre d'Etudies de Cramat (Lot)- France.

63. H. Conze, Desequilibre Electronique Dans un Choc, Scientific Report S-70-3, Centre d'Etudies de Gramat (Lot) - France.

64. P. Harris, Bull. Amer. Phys. Soc. 12, 840 (1967).

65. J. Y. Wong et al, Bull. Amer. Phys. Soc. 13, 1662 (1968).

66. Y. Horie, J. of Engineering Math. 3, 55 (1969).

67. A. L. Fuller and R. A. Gross, Phys. Fluids 11, 534 (1968).

68. A. Bauer et al, Ionization in the Shock Initiation of Detonation. Dept. of Metallurgy, University of Utah, Salt Lake, Utah. Sept 1962, Contract AF-18 (603) - 100.

69. H. S. Green, <u>Magnetrohydrodynamic Theory of Deflagration and Detonation.</u> U. S. Naval Ordnance Test Station, China Lake, California. NAVWEPS Report 8132, March 1964.

70. F. Williams in <u>Chemical Dynamics: Papers in Honor of Henry Eyring</u>, Edited by J. O. Hirschfelder (John Wiley & Sons, New York, 1971).

71. For example, see C. S. Choi and H. P. Boutin, Acta Cryst. <u>B25</u>, 982 (1969).

72. E. R. Fitzgerald, J. Phys. Chem. Solids <u>30</u>, 2771 (1969).

73. M. Born and K. Huang, <u>Dynamical Theory of Crystal Lattices</u> (Clarendon Press, Oxford, 1954).